Proceedings of
The Second National Congress on Fluids Engineering
August 22-24, 2002, Muju, Korea

The wake flow control behind a circular cylinder using ion wind

K T Hyun* and C H Chun**

이온풍을 이용한 실린더 뒤의 후류 제어

현기탁* · 전중환**

Key Words *: wake , ion wind, EHD Number, corona discharge*

Abstract

Many active and passive flow control methods have been studied since decades, but there are only few works about flow control methods using ion wind. This paper presents an experimental study on the wake control behind a circular cylinder using ion wind, a bulk motion of neutral molecules driven by locally ionized air of corona discharge. Experiments are done for different electrohydrodynamic numbers - the ratio of an electrical body force to a fluid inertial force - from 0 to 2 and for the Reynolds number ranging from 4×10^3 to 8×10^3. Pressure distributions over a cylinder surface are measured and flow visualizations are carried out by smoke wire method. Flow visualizations confirm that ion wind affects significantly the wake structure behind a circular cylinder and pressure drag could be dramatically reduced by the superimposing ion wind.

1. Introduction

Flow control can be generally discussed two parts; One is boundary layer control such as boundary layer transition delay or advancement and prevention or provocation of boundary layer separation and skin friction reduction. The other one deals with wake control behind bluff bodies, which affects rather the wake structure and therewith the pressure distribution on the rear part of the bluff bodies. The pressure drag can be suppressed or enhanced by influencing the vortex shedding. The methods of boundary layer control and wake control could be divided again into two parts, passive methods with no auxiliary power and active methods. Active methods require energy input like suction, blowing, injection of micro-bubble or particles, acoustic wave, periodic rotation or oscillation and MHD force. Numerous researchers have been studying active control methods in recent years. But there are only few works for flow control methods using ion wind.

Ion wind discovered by Hauksbee (1719) was regarded as a curiosity for many years. The investigation by Chattock(1899) gives pressure distributions on the plate and showed that ion wind is a jet of gas whose order is 1 m/s. Leonard et al [1], Kallio and Stock [2] studied flow field with ion wind and the migration velocity of particles in a electrostatic precipitator. Fujino et al [3], Ohadi et al [4], Owsenek and Seyed-Yagoobi [5] studied heat transfer enhancement by ion wind.

Malik et al [6] studied ion wind effect on viscous drag numerically and reported that ion wind is to be several meters per second contributing to the momentum of boundary layer and a reduction in the drag. Rosendale et al [7] studied Poiseuille flow at low speeds comparable to ion drift velocity and reported that ion wind strongly affects the skin-friction distribution and results in the drag reductions of 20% for an applied voltage of 15 kV. Soetomo [8] experimentally investigated the drag effect for both AC and DC corona discharges on a small flat glass plate. El-khabiry and Colver [9] studied Corona-induced drag reduction numerically over a flat plate and predict the corona thinning of the boundary layer for a downstream ion flow and a corresponding reduction in drag.

Most previous works on corona discharges were focused on not the flow control but the flow in an electrostatic precipitator and heat transfer enhancement. Some studies on flow control was done by Malik et al (1983), Rosendale et al (1988), Soetomo (1992), El-khabiry and Colver (1997) and Roth et al (1998). Their researches are, however, about skin friction drag reduction of flow over a flat plate. Little attention was given yet to the wake flow control of bluff bodies except the studies of Artana et al (1999) and Leger et al (2001). Artana et al [10] studied on DC corona discharge in a wire-plate electrode configuration placed on the surface of an insulating cylinder. In this study, flow visualization showed that the wake was largely modified and controlled by ion wind. But Artana's work is focused on the characteristics of corona discharge around a cylinder. Leger et al [11] measured the velocity around an inclined flat plate by PIV and flow visualizations showed that ion wind might have a high influence on the flow patterns and a separated airflow was reattached to the plate and wake size and drag were reduced, but didn't comment on the quantities of drag reduction. In this paper, the quantities of drag reduction are measured.

The purpose of this paper is to study the wake flow control of a circular cylinder using ion wind. For this, the pressure distributions on cylinder surface are measured and wake flow is visualized using smoke wire in changing the location of electrodes and N_{EHD}.

2. Description of experiments

Experiments were carried out in a low-speed open-circuit wind tunnel. The dimensions of duct are 30 cm in width, 40 cm in height and 100 cm in length. The wind tunnel has a maximum velocity of 2.5m/s and velocity distribution at the test section is uniform with a uniformity of 2 % of the free-stream velocity and the turbulence intensity is 1.5 % of the free-stream velocity measured by a hot wire. A hole of diameter D =61mm was made at the center of two sidewalls in the test section. A smooth circular cylinder of diameter D=60 mm is positioned horizontally through the holes of both walls of the test section, spanning the axis normal to the flow. Forty-eight pressure holes were made at 7.5-degree intervals on the mid vertical plane of the cylinder.

The area blockage ratio is 15% and the aspect ratio is 5. A cylinder is made a little big for adequate voltage-current characteristics and the simple installation of electrodes and making forty-eight pressure taps over the cylinder surface. The correction for blockage was done by Ota's correction formula [12] suitable for high blockage.

A thin aluminum tape was attached to whole cylinder surface for the ground electrode and a stainless steel wire with diameter of 0.09 mm was used for the high positive discharge electrode. The locations of

* POSTECH Mech. Eng., kthyun@postech.ac.kr
** POSTECH Mech. Eng., plume@postech.ac.kr

	A	B	C	D	E	F
θ	45°	90°	135°	180°	90°	90°
H	D/2	D/2	D/2	D/2	D/4	D/6

Table 1. Locations of electrodes

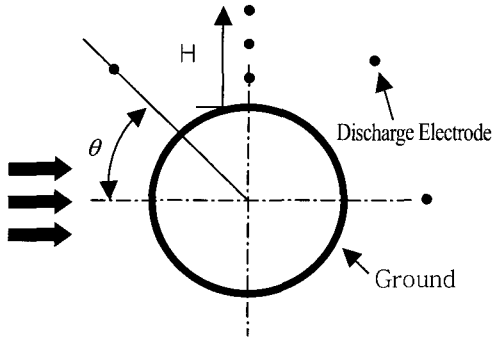

Fig. 1 the locations of electrodes

electrode wires for each experiment are shown Fig. 1 and Table 1: four places according to the change of angle and 2 more places according to the change of wire-to-cylinder spacing. Wire electrodes were connected to the high voltage (0-50 kV), low current (0-5 mA) DC power supply with positive polarity. Pressure measurements were taken over one-half azimuth of a cylinder after careful determination of a stagnation position. Differential pressure transducer was used to measure pressure with dual maximum range for differential pressure (±2pa, ±20pa).

Flow visualizations were conducted using a vertical smoke-wire system at the free-stream velocity of 1 m/s. A smoke-wire was made of stainless steel which diameter was 0.09 mm. A 5W Argon-ion laser was used for light sheet and a digital camera was used for capturing photographic images.

3. Results and discussion

Electrohydrodynamic number N_{EHD} is a very important nondimensional parameter in electro-hydrodynamics phenomena, which is equal to the ratio of an electrical body force to a fluid inertial force (Davidson and Shaughnessy [13]). N_{EHD} is calculated according to

$$N_{EHD} = \frac{I\,H}{\rho\,U_0^{\,2}\,\beta\,A}$$

The pressure drag coefficient Cd is calculated according to

$$Cd' = \frac{D_P}{1/2\,\rho U_0^{\,2}\,A_p}$$

And then, the correction for blockage was done by Ota's formula. D_P is pressure drag and is calculated using surface pressure of a cylinder.

(I: current, H: Electrode spacing, β : ion mobility, A : area of ground electrode, D_p: Pressure drag, A_p: projected area)

3.1 Effect of installation angle

At first experiments were done in changing installation angle of wire electrodes (θ). Fig. 2 shows Cp distributions according to the change of N_{EHD} at θ= 45°, θ= 135° and θ= 180°. From Cp distribution (Fig. 2) and flow visualization (Fig. 3), it is evident that ion wind can change pressure distribution and drag and flow structures. As positive ions moves flows along a electric line, ion wind give a momentum a different position according to θ variation, and flow patterns are quietly different one another as shown in Cp distribution and flow visualizations.

At θ= 45°, positive ions generated by corona discharge move along a electric characteristic line and give their momentum fluid between discharge electrodes and a cylinder during movement. With N_{EHD} increased, more momentum is transferred to fluid; therefore this makes separation point move gradually rearward as shown in Fig. 2. Flow visualizations show clearly that flow separation point is already over θ=

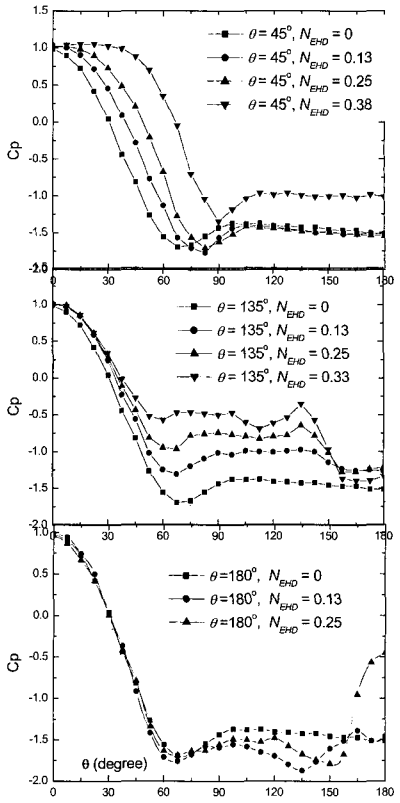

Fig. 2 Cp curves according to the N_{EHD} at H= D/2, U = 1m/s.

90° at N_{EHD}=0.25 and ion wind goes toward to a cylinder surface at N_{EHD} =0.5. The delay of flow separation makes a wake width decreased. This change of flow structure also leads to suppress the periodic vortex

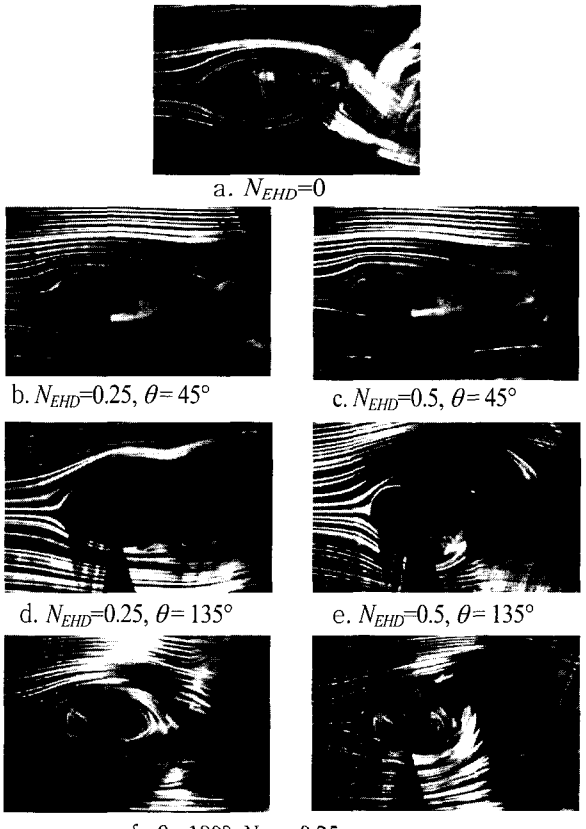

Fig. 3 Flow visualizations with change of N_{EHD} according to the installation angle (45°, 135°, 180°), U_0= 1m/s, H= D/2.

shedding and this implies the suppression of the lift force oscillation and a cylinder vibration.

Different phenomena happen when discharge electrodes are at θ = 135°. Ion wind makes a stagnation point at θ = 135° and pushes fluid toward the upstream against the flow making a recirculation flow at the upper and lower sides of a cylinder. As a result of it, separation point moves gradually to the fore part of the cylinder and a wake width grows larger with N_{EHD} increase. Pressure peak by the influence of ion wind is clearly seen at θ = 135° in Fig. 2 in increasing N_{EHD}.

When the discharge electrode is at θ = 180°, ion wind amplifies vortex shedding and makes bigger and regular vortex shedding than the case without electric field as seen in Fig. 3. It is effective to disturb the flow and enhance the mixing of the flow and a heat transfer. Fig. 2 shows that a base pressure is increased according to the increase of N_{EHD}.

Flow structures can be controlled by the change of locations of discharge electrodes (θ = 45°, 135°, 180°). It is possible to suppress or enhance the vortex shedding and make a wake width small or large, but *Cd* is a little changed because of two effects of ion wind. One positive effect is the delay of flow separation and the negative is the increase of frontal pressure by giving the momentum of ion wind to fore part of a cylinder.

3.2 Effect of wire-to-cylinder spacing on *Cp* and *Cd* distribution

Experiments were carried out for three different wire-to-cylinder spacing (*H*= D/2, *H*= D/4, *H*= D/6) in the case of θ = 90°.

According as N_{EHD} is increased, three different flow characteristics are observed in the case of θ = 90°. At low N_{EHD} when a flow inertia force is stronger than EHD force, ion wind does not directly flow toward a cylinder, namely, no another stagnation point. When the strength of EHD force is similar with the strength of a flow inertia force, a stagnation point comes out at about θ = 97.5°. At relatively high N_{EHD}, EHD force is so great that the stagnation flow from discharge electrodes to a cylinder can be clearly observed from the flow visualization and the pressure peak occurs at θ = 97.5°. The recirculation flow is formed at the upper and the lower of a cylinder.

Fig. 4 is *Cpb* distribution according to wire-to-cylinder spacing. Three different patterns appear. *Cpb* is increased according to the increase of N_{EHD} at low N_{EHD} and then not increased in spite of the increase of N_{EHD} and reincrease according to the increase of N_{EHD} at relatively high N_{EHD}. The same pattern can be shown in *Cd* distributions of Fig. 5 because *Cd* is very closely related to *Cpb*.

A flow regime can be divided by N_{EHD}, but the N_{EHD} dividing the regime is dependent on the wire-to-cylinder spacing (*H*). Hereafter the

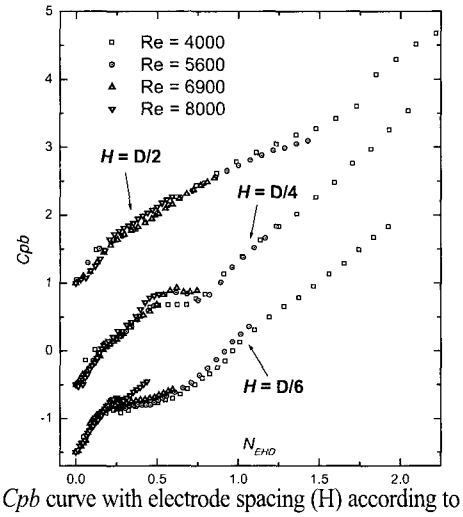

Fig. 4 *Cpb* curve with electrode spacing (H) according to N_{EHD} at θ = 90°(curve of *H*=D/4 is shifted up 1, 2.5 for *H*=D/2).

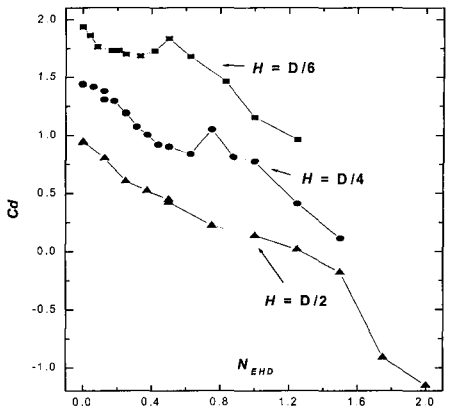

Fig. 5 *Cd* curve with wire-to-cylinder spacing according to N_{EHD} at θ = 90°. The curve of *H*=D/4 is shifted up 0.5 and 1 for *H*=D/6

N_{EHD} to divide a flow regime is named the critical N_{EHD}. As wire-to-cylinder spacing increases critical N_{EHD} increased. In a Fig. 4 and a Fig. 5, a second regime appears between N_{EHD}=0.2 and 0.5 at *H*=D/6, between N_{EHD}= 0.5 and 0.7 at *H* = D/4, but critical N_{EHD} is not distinctly seen at *H*=D/2. It seems to be between N_{EHD}= 1 and 1.5.

Though critical N_{EHD} is different according to wire-to-cylinder spacing, the tendencies of *Cd* and *Cpb* according to the change of N_{EHD} are consistent each other. The surprising thing is that *Cd* is negative, namely, no drag at about N_{EHD} = 1.2 for *H*= D/6, 1.19 for *H*= D/4 and 1.27 for *H*= D/2.

Fig. 6 show the *Cp* distributions of a cylinder. They show why the peak of *Cd* occurs at second regime and why second regime is indistinct in the case of *H* = D/2 and why the critical N_{EHD} is different according to wire-to-cylinder spacing.

As N_{EHD} is increased, irrespective of wire-to-cylinder spacing, base pressure is increased at the beginning. At first regime, positive ions doesn't give sufficient momentum to fluid to make a stagnation flow. The given momentum raises base pressure and *Cd* results in a decrease. At second regime, stagnation flow happens and this makes front pressure increase faster than the base pressure according to increase of N_{EHD}. So *Cd* is increased and the peak of *Cd* distribution could be seen. After fast increase of front pressure, momentum given by ions raises the base pressure and makes pressure peak seen clearly at θ = 97.5° at third regime. So *Cd* decreases according to the increase of N_{EHD}. Because

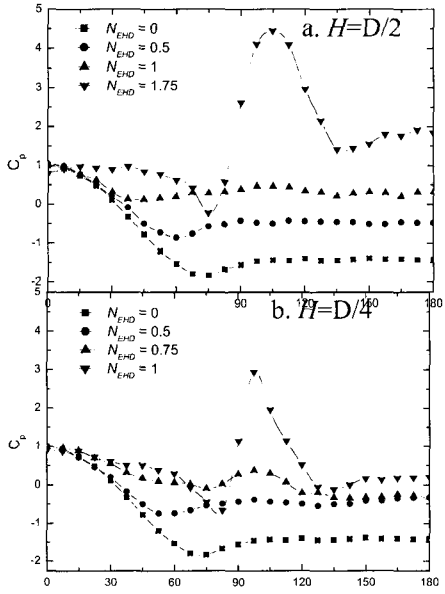

Fig. 6 *Cp* with N_{EHD} according to electrode spacing at θ = 90°

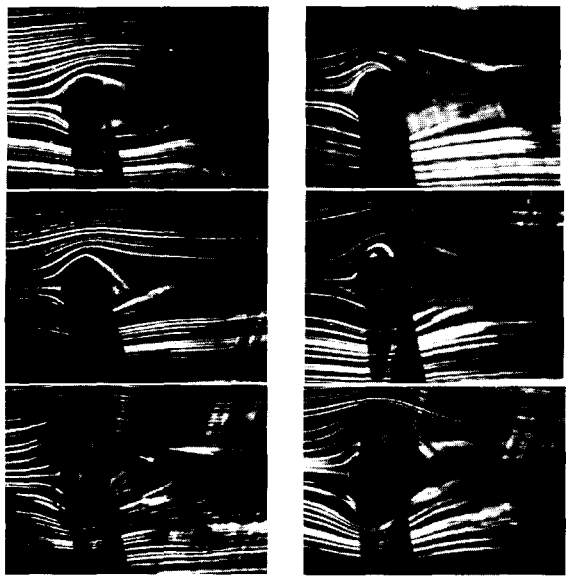

a. H=D/4 b. H=D/2

Fig. 7 Flow visualizations with N_{EHD} increase (N_{EHD} =0.25, 0.5, 1 for H= D/4, N_{EHD} =0.5, 1, 1.5 for H= D/2), θ= 90°, U_0= 1m/s

main flow convects ion wind a little downstream, the stagnation point is not located at θ= 90° but shifted to about θ= 97.5°. The pressure peak by the influence of ion wind is clearly seen at about θ = 97.5° in C_p distribution.

As wire-to-cylinder spacing increases, ion wind becomes larger and influences more wide surfaces of a cylinder, and more energy must be added to make a stagnation flow. As a result of it critical N_{EHD} increases and the momentum of ions raises not only the frontal pressure but also the base pressure at second regime in the case of H= D/2. So no peak in Cd appears and the critical N_{EHD} dividing flow regime at H= D/2 is indistinct.

3.34 Flow visualization in the case of θ= 90°

Flow visualization shows three flow patterns with N_{EHD} increased when wire-to-cylinder spacing is D/4 and D/2 respectively. Fig. 7a (N_{EHD}=0.25) and 7b (N_{EHD}=0.5) show flow pattern that flow inertia force is stronger than EHD force. Flow separation happens at the rear of a cylinder and the intensity of vortex shedding becomes weak. Fig. 7a (N_{EHD}=0.5) and 7b(N_{EHD}=1) show that stagnation flow happens and vortex shedding is not clearly seen. If EHD force become dominant, in Fig. 7a (N_{EHD}=1) and 7b (N_{EHD}=1.5) a stagnation flow can be seen surely and the recirculation flow is formed at both the upper and the lower of a cylinder by the resultant of ion movement and free stream. Vortex shedding is suppressed by ion wind and stagnation point appears at about θ= 97.5°.

4. Conclusions

Experiments were done by changing the installation angle of wire electrodes and wire-to-cylinder spacing for $0 \leq N_{EHD} \leq 2$ in Reynolds number range from 4×10^3 to 8×10^3.

At θ= 45°, with N_{EHD} increased separation point moves gradually rearward and wake width becomes smaller. At θ= 135°, separation point moves gradually forward and wake width grows larger. At θ= 180°, ion wind amplifies vortex shedding and makes bigger and regular vortex shedding. Flow structures could be controlled by ion wind, but Cd is a little changed because of the contrary effect of ion wind.

In the case of θ = 90°, according to the increase of N_{EHD} three different flow regimes are observed. At relatively low N_{EHD}, EHD force is too small to make a stagnation point on a cylinder, but pressure drag is decreased because of the increase of base pressure by ion wind. In the second regime, the strength of EHD force is large to make stagnation point seen at about θ= 97.5°. But pressure drag is not decreased because ion wind raises the front pressure of cylinder after a formation of stagnation point. At relatively high N_{EHD} where EHD force becomes dominant, stagnation flow can be clearly seen and the recirculation flow is formed at the upper and the lower of a cylinder. Pressure drag is decreased because base pressure is increased and much momentum is given directly to the stagnation point of a cylinder.

From this experiment it is shown that ion wind is useful for an active control of the wake flow including vortex shedding and flow separation. Ion wind could be used to reduce the pressure drag of a circular cylinder.

References

[1]Leonard GL; Mitchner M; Self SA An experimental study of the electrohydrodynamic flow in electrostatic precipitators. J Fluid Mech 127(1983), 123-140

[2]Kallio GA; Stock DE Interaction of electro-static and fluid dynamic field in wire-plate electrostatic precipitators. J Fluid Mech Vol. 240(1992), 133-166

[3]Fujino T; Yokoyama Y; Mori YH Augmentation of laminar forced convection heat transfer by application of a transverse electric field. J Heat Transfer 111(1989), 345-351

[4]Ohadi MM; Sharaf N; Nelson DA Electro-hydrodynamic enhancement of heat transfer in a shell-and-tube heat exchanger. Exp Heat Trans 4 (1991), 19-39

[5]Owsenek BL, SeyedYagoobi J Theoretical and experimental study of electrohydrodynamic heat transfer enhancement through wire-plate corona discharge J Heat Transfer-Trans of ASME 119 (3) (1997), 604-610

[6]Malik MR; Weinstein LM; Hussaini MY Ion wind drag reduction. AIAA paper 83-0231 (1983)

[7]Rosendale JR; Malik MR; Hussaini MY Ion-wind effects on poiseuille and blasius flow. AIAA journal 26(1988), 961-968

[8]Soetomo F The influence of high voltage discharge on flat plate drag at low Reynolds number airflow. M. S. thesis, Iowa Uni. Ames (1992)

[9]Colver G; El-Khabiry S Modeling of the corona discharge along an electrically conductive flat with gas flow. IEEE Trans. Ind. Appl., Vol. 35(1999), 387-394

[10]Artana G; Desimone G; Touchard G Study of the changes in the flow around a cylinder caused by electroconvection. Electrostatics 1999 Ins Phy Conf. Ser. Vol 163 (1999), pp 147-152

[11]Leger L; Moreau E; Artana, G; Touchard G Influence of a DC corona discharge on the airflow along an inclined flat plate. J Electrostatics 51-52(2001), 300-306

[12]Ota T; Okamoto Y; Yshikawa H A correction formula for wall effects on unsteady forces of two-dimensional bluff bodies. Trans of ASME 12(1994), 414-418

[13]Davidson JH; Shaughnessy EJ Turbulence generation by electric body forces. Exp Fluids 4 (1986), pp 17–26